

Behavior of symmetrically haunched non-prismatic members subjected to temperature changes

S. Bahadir Yuksel[†]

Department of Civil Engineering, Selcuk University, Konya, Turkey

(Received September 17, 2007, Accepted January 12, 2009)

Abstract. When the temperature of a structure varies, there is a tendency to produce changes in the shape of the structure. The resulting actions may be of considerable importance in the analysis of the structures having non-prismatic members. Therefore, this study aimed to investigate the modeling, analysis and behavior of the non-prismatic members subjected to temperature changes with the aid of finite element modeling. The fixed-end moments and fixed-end forces of such members due to temperature changes were computed through a comprehensive parametric study. It was demonstrated that the conventional methods using frame elements can lead to significant errors, and the deviations can reach to unacceptable levels for these types of structures. The design formulas and the dimensionless design coefficients were proposed based on a comprehensive parametric study using two-dimensional plane-stress finite element models. The fixed-end actions of the non-prismatic members having parabolic and straight haunches due to temperature changes can be determined using the proposed approach without necessitating a detailed finite element model solution. Additionally, the robust results of the finite element analyses allowed examining the sources and magnitudes of the errors in the conventional analysis.

Keywords: non-prismatic member; finite element analysis; fixed-end force; temperature effects.

1. Introduction

Bridges and buildings often contain non-prismatic members identified with a varying depth along their span lengths. Commonly, linear or parabolic height variations are selected to lower the stresses at the high bending moment points and to maintain the deflections within the acceptable limits. Fig. 1 demonstrates a single span bridge having symmetrical parabolic haunches.

In 1958, Portland Cement Association issued the "Handbook of Frame Constants (PCA 1958)" that contains a series of tables listing the carryover factors, stiffness factors, and fixed-end moment coefficients for commonly used non-prismatic members, which were derived by using some crude assumptions at the time to simplify the problem (El-Mezaini *et al.* 1991). It should be pointed out that, the fixed-end actions due to temperature changes were not published in those PCA tables. These factors have been used in the conventional methods since 1958 for the analyses of the non-prismatic members by utilizing the moment distribution method and the slope deflection method (Maugh 1964, Timoshenko and Young 1965, Tardaglione 1991, Hibbeler 2002). The results of the finite element analyses performed by El-Mezaini *et al.* (1991) proved that the fixed-end moments,

[†] Professor, Corresponding author, E-mail: sbahadiryuksel@yahoo.com



Fig. 1 A typical single span bridge having symmetrical parabolic haunches

the bending stiffness and the carry-over factors for the non-prismatic members given in PCA (1958) involve significant errors, especially for deep haunches.

The elastic modeling of the non-prismatic members evolved after the publication of the PCA handbook of the frame constants (PCA 1958) and caught the attention of a few researchers in the last four decades (Tena-Colunga 1996). Eisenberger (1985) derived the explicit stiffness matrices of several common non-prismatic members from the flexibilities of the elements without considering any shear deformations. Vanderbilt (1978) and Funk and Wang (1988) calculated the stiffness matrix and the fixed-end forces by dividing the non-prismatic member into sub-elements. Medwadowski (1984) solved the bending problem of the non-prismatic shear beams in terms of a displacement function, which was based on the calculus of variations. Brown (1984) presented a method in which the approximate interpolation functions consistent with the beam theory and the virtual work principle were used to obtain the stiffness matrix for tapered beams. Eisenberger (1991) derived the exact terms of the stiffness matrix for the non-prismatic members including shear deformations from the flexibilities of the element. El Mezaini *et al.* (1991) investigated the linear elastic behavior of the frames with non-prismatic members by using the isoparametric plane stress finite elements. Friedman and Kosmatka (1992a) derived the exact axial, bending and torsion stiffness matrices for an arbitrary non-uniform Bernoulli-Euler beam element, where the effects of the shear deformations were neglected. Friedman and Kosmatka (1992b) developed the exact bending stiffness matrix for an arbitrary non-uniform beam, which was based upon the Timoshenko's beam theory in which the shear deformation is accounted for. Al-Gahtani (1996) derived the stiffness matrix by using differential equations and the boundary integral method, and determined the fixed-end forces for the distributed and concentrated member loads. Tena-Colunga (1996) presented the stiffness matrices for linearly tapered members while accounting shear deformations based on the traditional Bernoulli-Euler beam theory. Ozay and Topcu (2000) proposed a general stiffness matrix for the non-prismatic members, which is applicable to Bernoulli-Euler and Timoshenko beam theory. Balkaya (2001) investigated the behavior of the non-prismatic members having T-sections and computed the fixed-end moments, the bending stiffness coefficients and the carry-over factors from the three-dimensional finite element models by considering the thrust effects. El Mezaini *et al.* (1991) and Balkaya (2001) proved that the conventional method of analysis for the non-prismatic structures leads to erroneous results and the deviations reach to unacceptable levels for these types of structures with deep haunches. Other researchers have recently provided many test results about the haunched beams (Shanmugam *et al.* 2002, Tanaka 2003, Lee *et al.* 2003, Hu *et al.* 2006, Pampanin

et al. 2006, Oh *et al.* 2007). Unfortunately, the behavior of the non-prismatic members subjected to temperature changes was not considered in all these studies. To the writer’s knowledge, the effects of the temperature changes on the non-prismatic members have not been investigated by using the finite element analysis so far.

The purpose of this paper is to investigate the behavior of the non-prismatic beams having linear and parabolic haunches due to uniform and non-uniform temperature changes. In this conjunction, the present study carried out many finite element analyses for various non-prismatic beams having different haunch lengths and haunch depths. To produce benchmark results for the finite element analyses, four-node isoparametric plane-stress finite elements with two translational degrees of freedom (d.o.f.) and one rotational d.o.f. per node were utilized for modeling various non-prismatic beams. The fixed-end moments and the fixed end forces of the non-prismatic members having symmetrical linear and parabolic height variations were computed under the action of temperature changes. This paper advances to propose effective formulas and dimensionless design coefficients to predict the bending moments and the axial forces with reasonable accuracy for the non-prismatic members subjected to temperature changes.

2. The end-actions for the restrained prismatic members subjected to temperature changes

A restrained member is the one whose ends are restrained against the translational and rotational displacements, as in the case of a fixed-end beam. The end-actions for the restrained members subjected to the temperature changes are the reactive actions (fixed-end forces and fixed-end moments) developed at the ends. Many classical books on structural analysis (Weaver and Gere 1990, Tartaglione 1991, Hibbeler 2002) give the fixed-end actions of the prismatic members under temperature changes. The fixed-end actions of a prismatic beam with a rectangular cross-section of $b \times h$ and length L under uniform and non-uniform temperature changes are given in Fig. 2(a) and Fig. 2(b), respectively. Eq. (1) is for a beam subjected to a uniform temperature increase of ΔT . The resultant end-actions consist of only the axial compressive forces that are independent of the beam length of the member. Eq. (2) is for a beam subjected to a linear temperature gradient (non-uniform temperature changes) such that the top of the beam has a temperature change of ΔT_2 while the bottom has a change of ΔT_1 . If the temperature at the centroidal axis remains unchanged, the length of the beam will not tend to change and the end-actions will consist of moments only. On the other hand, Eq. (1) covers a nonzero change of temperature at the centroidal axis. The formulas given in Eq. (1) and Eq. (2) can be derived by using the standard methods of mechanics of materials and also by the flexibility method.

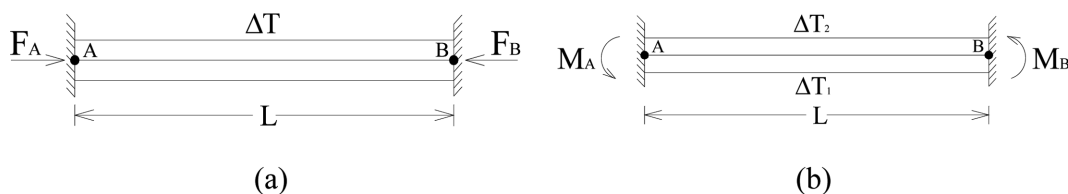


Fig. 2 Fixed-end actions of the prismatic beams subjected to (a) uniform temperature changes (b) linear temperature gradient (non-uniform temperature changes)

$$F_A = -F_B = F = \{E \times A \times \alpha T \times \Delta T\} \tag{1}$$

$$M_A = -M_B = M = \frac{\alpha T \times E \times I \times (\Delta T_1 - \Delta T_2)}{h} \tag{2}$$

Where F is the fixed-end horizontal force at the ends of the prismatic member under uniform temperature changes, M is the fixed-end moment at the ends of the prismatic member under non-uniform temperature changes, E is the modulus of elasticity, A is the cross-sectional area, αT is the coefficient of thermal expansion, L is the length of the member, ΔT is the uniform temperature change (positive sign means increase in temperature), I is the moment of inertia, ΔT_1 is the temperature change at the bottom of the beam, ΔT_2 is the temperature change at the top of the beam, $(\Delta T_1 - \Delta T_2)$ is the linear temperature gradient, and h is the mid-span depth of the beam.

3. The end-actions for the restrained non-prismatic members subjected to temperature changes

The behavior of the non-prismatic members differs from that of prismatic ones in terms of the variation of the cross-section along the member, the continuous change in the centroidal axis associated with the non-prismatic section, the nonlinear stress distributions over the cross sections and the arching action effect (El-Merzaini *et al.* 1991, Balkaya 2001). The geometric parameters of the non-prismatic beams with symmetrical parabolic haunches are presented in Fig. 3; where, L is the length of the beam, b is the width of the beam, h is the mid-span or minimum depth of the non-prismatic element, α is the haunch length ratio (haunch length over the total length of the member), R is the haunch depth ratio.

Uniform temperature change produces axial force reactions only in the prismatic members as shown in Fig. 2(a), whereas, in addition, bending moments also develops in the non-prismatic members as shown in Fig. 4(a). It is obvious that the continuous change of the centroidal axis of the non-prismatic members causes strong coupling between the bending moments and the axial forces. F_{UT} is the fixed-end horizontal force and M_{UT} is the fixed-end moment for the non-prismatic member under uniform temperature change. Furthermore, if a prismatic member is subjected to a linear temperature gradient such that the top of the beam has a temperature change of ΔT_2 , while the bottom has a change of ΔT_1 and the temperature at the centroidal axis remains unchanged, only the bending moments occur as shown in Fig. 2(b). However, the axial forces are developed in addition to the bending moments (see Fig. 4(b)) at the ends of the non-prismatic members for the

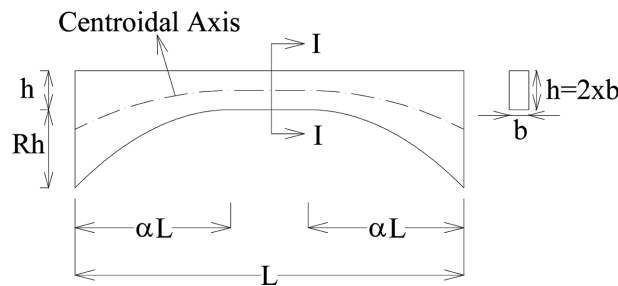


Fig. 3 Geometric parameters of a typical non-prismatic beam with parabolic haunches

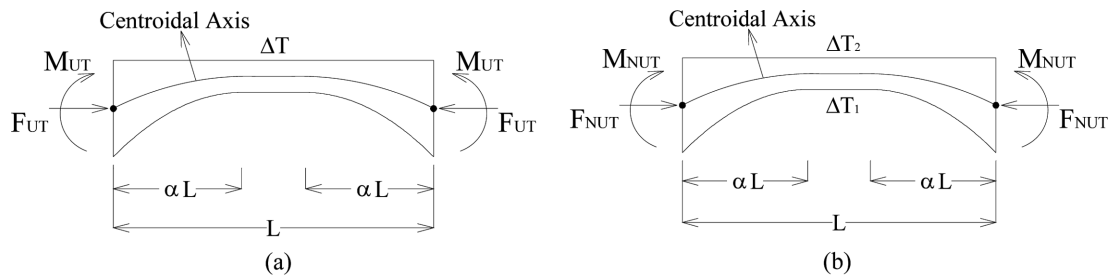


Fig. 4 Fixed-end forces and the fixed-end moments of the non-prismatic members under the conditions of; (a) uniform temperature increase (ΔT), (b) linear temperature gradient ($\Delta T_1 - \Delta T_2$)

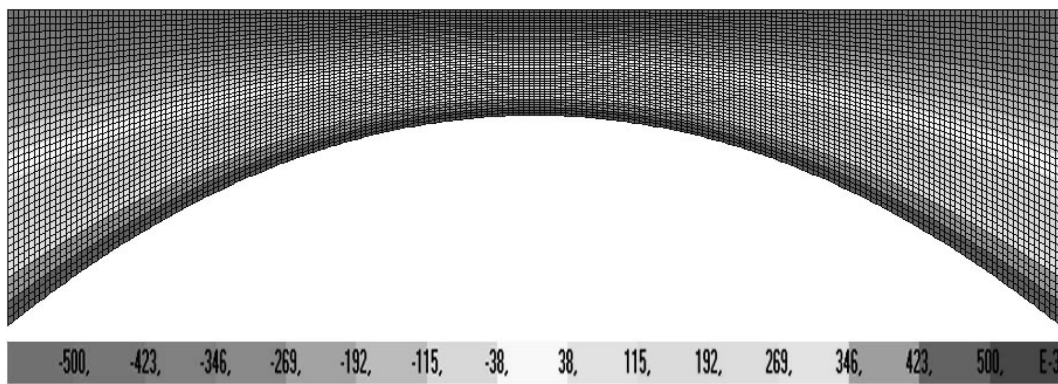


Fig. 5 Application of the linear temperature gradient to the non-prismatic members such that $\Delta T_2 = -0.5$ and $\Delta T_1 = 0.5$ ($\Delta T_1 - \Delta T_2 = 1C^\circ$) and the temperature at the centroidal axis remains unchanged

same situation. F_{NUT} is the fixed-end horizontal force and M_{NUT} is the fixed-end moment at the ends of the non-prismatic members under non-uniform temperature changes ($\Delta T_1 - \Delta T_2$). By using the finite element models of the non-prismatic members, the F_{UT} and M_{UT} values were calculated under the actions of $\Delta T = 1C^\circ$ temperature increase, and additionally the F_{NUT} and M_{NUT} values were calculated under the actions of the linear temperature gradient of $\Delta T_1 - \Delta T_2 = 1C^\circ$. Fig. 5 shows the application of the linear temperature gradient to non-prismatic members such that the top of the beam has a temperature change of $\Delta T_2 = -0.5$, while the bottom has a temperature change of $\Delta T_1 = 0.5$ ($\Delta T_1 - \Delta T_2 = 1C^\circ$) and the temperature at the centroidal axis remains unchanged.

4. The assumptions for the development of the analytical model and the parametric study

The non-prismatic beams with symmetric parabolic haunches and straight haunches of varying haunch depths and haunch lengths were generated as the model structures of the analysis. The non-prismatic beam members of rectangular cross section ($b \times h$) and length L were assumed to be made up of homogeneous, isotropic and linearly elastic material. The geometrical configuration given in Fig. 3 was used for the analyses of the non-prismatic beams with varying haunch depths and haunch lengths.

In all of the analyses, the beam lengths ($L = 10$ m), the beam widths ($b = 0.5$ m) and the mid-span

depths ($h = 1$ m) of the non-prismatic elements were taken as constant while the other values were changed to achieve the parameter values. Modulus of Elasticity (E) and the Poisson's ratio (ν) were taken as 3×10^7 kN/m² and 0.2, respectively. The parametric studies were performed on the non-prismatic beams having straight and parabolic haunches with varying haunch depths and haunch lengths. The haunch length coefficients ($\alpha = 0.1, 0.2, 0.3, 0.4$ and 0.5) and the haunch depth coefficients ($R = 0.0, 0.1, 0.2, 0.3, 0.4, 0.5, 0.6, 0.7, 0.8, 0.9, 1.0, 1.1, 1.2, 1.3, 1.4, 1.5, 1.6, 1.7, 1.8, 1.9$ and 2.0) were varied for both the parabolic and the straight haunched non-prismatic beams. The combination of all these values resulted in 210 non-prismatic beams having parabolic and straight haunches different from each other in geometry. The uniform and non-uniform temperature changes were applied to each non-prismatic beam having parabolic and straight haunches. Therefore, in total, 420 finite element analyses were carried out to calculate the fixed-end actions of the non-prismatic beams. The developed fixed-end moments and the fixed-end horizontal forces due to uniform and non-uniform temperature changes were calculated by using the finite elements models. The results were next used in developing the design equations and the estimator coefficients.

5. The finite element modeling of the non-prismatic members

The behavior of the non-prismatic members having symmetrical haunches was investigated by developing two dimensional finite element models using SAP2000 (CSI 2007a). To produce benchmark results for the finite element analyses, four-node shell elements with two translational degrees of freedom (d.o.f.) and one rotational d.o.f. per node were utilized for the modeling of various non-prismatic beams having different haunch depths and haunch lengths. Especially, the modeling of the non-prismatic members with parabolic haunches is complicated by the fact that the bottom face of these members has parabolic shape variations. There is no parabolic node generation option for the most commonly used commercial software such as SAP2000 (CSI 2007a). For that reason, a preprocessor was prepared to be able to generate the finite element models of the non-prismatic members. The typical finite element models for the non-prismatic beams can be seen in Figs. 5, 6 and 7. In order to satisfy the adequate accuracy for the results of the finite element analyses, each non-prismatic beam was divided into 8000 elements.

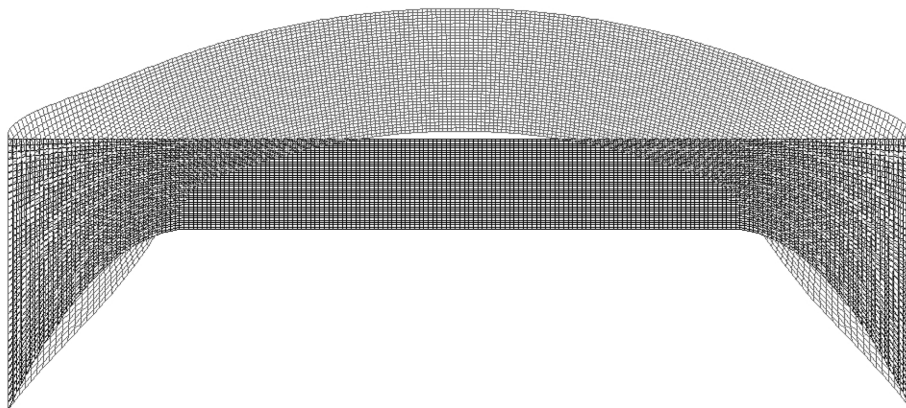


Fig. 6 A typical exaggerated deflected shape of a 10 m long non-prismatic beam having parabolic haunches with $\alpha = 0.2$ and $R = 2$ due to $\Delta T = 1\text{C}^\circ$ uniform temperature increase

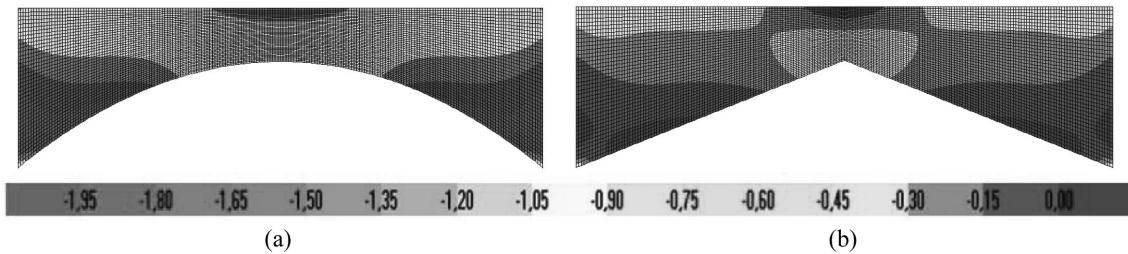


Fig. 7 Axial stress contours for the non-prismatic beams ($b = 0.5$ m, $h = 1$ m, $L = 10$ m, $\alpha = 0.5$ and $R = 2$) having (a) parabolic haunches (b) straight haunches due to $\Delta T = 1\text{C}^\circ$ uniform temperature increase (units are in kN/m^2)

The results obtained by the finite element analyses can be accepted as the real elastic values. The actual behavior of the non-prismatic members can be accurately simulated with the finite element model used in this study and El-Mezaini *et al.* (1991). The discontinuity of the centroidal axis, the local stress concentrations, the nonlinear stress distributions and the existence of null areas that reduces the member stiffness are taken into consideration in both of the models. Since the stress concentrations, non-uniform stress distributions, the coupling between the axial forces and the moments were not considered in the classical beam theory, the approximate results obtained from the beam theory deviated from the real elastic values.

The fixed-end forces and the fixed-end moments of the non-prismatic members due to temperature changes were obtained by using the finite element analyses. The computation of the stress values or nodal forces is not sufficient for the calculation of the fixed-end actions. Despite the robustness of the finite element modeling, the generation of the fixed-end moments and the fixed-end forces from the nodal outputs of the detailed mesh still remains as an intricate task. The fixed-end forces and the fixed-end moments due to temperature changes were calculated using the nodal force outputs of the finite element analyses proposed by Bathe (1996) and applied as in Horowitz (1997), Balkaya *et al.* (2006), Yuksel (2008), and Yuksel and Arıkan (2009). The postprocessor was developed to sum the nodal point element forces at the predetermined sections in order to be able to calculate the fixed-end actions.

6. General behavior of the non-prismatic members subjected to temperature changes

Variation of the cross-section parameters affects the location of the neutral axis, and the rigidity of the section. Thus, being important in the arch formation, they respectively affect the location of the arch length, arch height and the general behavior of the non-prismatic members subjected to temperature changes. A typical exaggerated deflected shape of a 10 m long non-prismatic beam having parabolic haunches with $\alpha = 0.2$ and $R = 2$ under $\Delta T = 1\text{C}^\circ$ uniform temperature increase is illustrated in Fig. 6. The non-prismatic beam deflected in the upward direction under the uniform temperature increase of $\Delta T = 1\text{C}^\circ$. The continuous change in the centroidal axis associated with the non-prismatic sections causes a strong coupling between the bending moments and the axial forces. In Fig. 7(a), the axial stress contours due to $\Delta T = 1\text{C}^\circ$ uniform temperature increase via the finite element method are shown for the parabolic haunched beams (given $b = 0.5$ m, $h = 1$ m, $L = 10$ m, $\alpha = 0.5$ and $R = 2$). In Fig. 7(b), the same plot is shown for a straight haunched beam (given $b =$

0.5 m, $h = 1$ m, $L = 10$ m, $\alpha = 0.5$ and $R = 2$). The comparison of Figs. 7(a) and 7(b) stated that the distribution of the stresses differed in each non-prismatic member depending on the manner of the variation of the cross-section. The stress distributions occurred so complex and nonlinear in the non-prismatic members subjected to temperature changes, which require special attention.

7. Evaluation of the design forces obtained by the finite element model

Fixed-end actions (F_{UT} , F_{NUT} , M_{UT} and M_{NUT}) were obtained using the finite element models under uniform and non-uniform temperature changes for different haunch depth ratios (R) and haunch length ratios (α). The plots were presented for the variations in the fixed-end horizontal forces and fixed-end moments as the functions of the haunch depth ratios ($R = 0.0, 0.1, 0.2, 0.3, 0.4, 0.5, 0.6, 0.7, 0.8, 0.9, 1.0, 1.1, 1.2, 1.3, 1.4, 1.5, 1.6, 1.7, 1.8, 1.9$ and 2.0) for different values of haunch length ratios ($\alpha = 0.1, 0.2, 0.3, 0.4$ and 0.5).

The results of the finite element analyses performed to investigate the fixed-end forces (F_{UT}) under the action of the uniform temperature increase of $\Delta T = 1C^\circ$ for the non-prismatic members having parabolic haunches and straight haunches were presented in Fig. 8(a) and Fig. 8(b), respectively. The results showed that for a given specific haunch depth ratio, as the haunch length ratios increase, the increase in F_{UT} occurs at an increasing rate. The relationship between the F_{UT} and the haunch depth ratio is nonlinear. For the haunch length ratios of $\alpha = 0.1$ and 0.2 , the F_{UT} increase for the non-prismatic members having parabolic and straight haunches up to $R = 0.6$ was reached, then the curves became flat. For the non-prismatic members having haunch length ratios of $\alpha = 0.3, 0.4$ and 0.5 , as R increases, the increase in the values of the F_{UT} decreases with an increasing rate. The uniform temperature changes influence the values of the F_{UT} for the non-prismatic members with straight haunches more than the values of those for the non-prismatic members with parabolic haunches.

The typical variations of the fixed-end moments (M_{UT}) of the non-prismatic members having parabolic haunches and straight haunches are presented in Fig. 9(a) and Fig. 9(b), respectively. From the finite element modeling, it is seen that the fixed-end moments occur at the ends of the non-prismatic beams under the uniform temperature changes. Because of the arching action in the non-prismatic members, the change of the centroidal axis produces fixed-end moments (M_{UT}) in

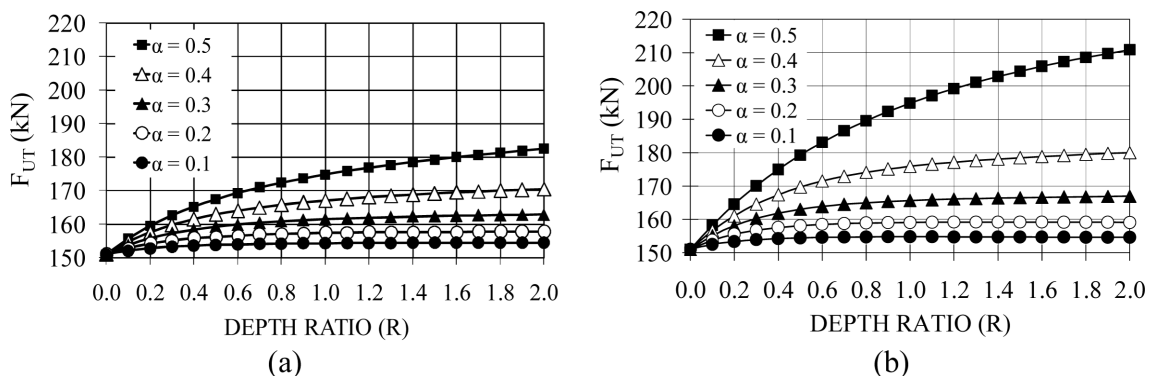


Fig. 8 Variation of the horizontal reaction forces (F_{UT}) of the non-prismatic members having (a) parabolic haunches, (b) straight haunches; under the action of uniform temperature increase of $\Delta T = 1C^\circ$

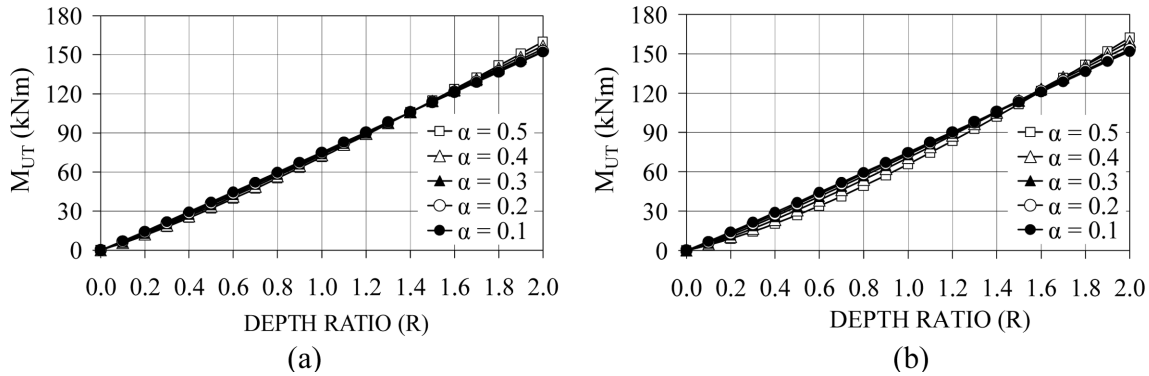


Fig. 9 Variation of the fixed-end moments (M_{UT}) of the non-prismatic members having (a) parabolic haunches, (b) straight haunches; under the action of uniform temperature increase of $\Delta T = 1C^\circ$

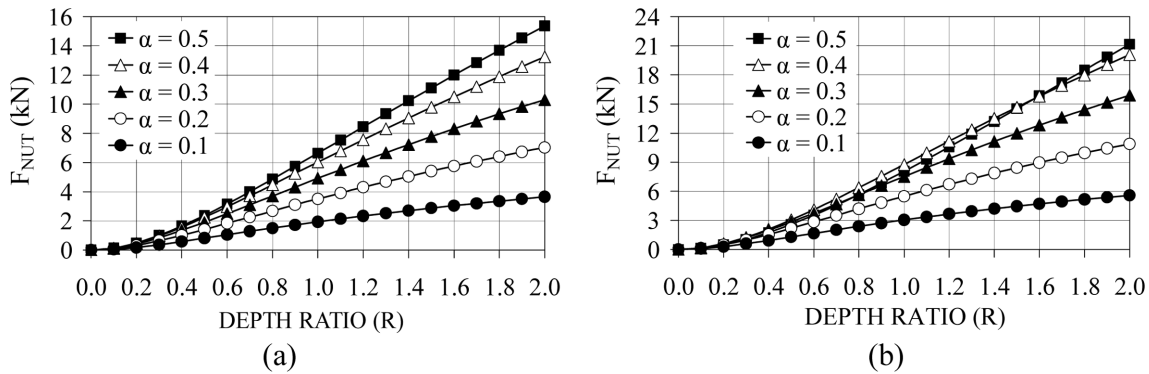


Fig. 10 Variation of the fixed-end horizontal forces (F_{NUT}) of the non-prismatic members having (a) parabolic haunches, (b) straight haunches; under the action of linear temperature gradient of $(\Delta T_1 - \Delta T_2 = 1C^\circ)$

addition to fixed-end forces (F_{UT}) under the actions of the uniform temperature increase when the ends of the non-prismatic members are restrained. For a given specific haunch length ratio, as the haunch depth ratio increases, the fixed-end moments increase linearly. The relationships between the values of M_{UT} and the haunch depth ratios are linear for parabolic and straight haunches. Also for a given specific haunch depth ratio, the fixed-end moments (M_{UT}) are almost same for different haunch length ratios. These fixed-end moments cannot be obtained by applying the conventional methods of analyses using frame elements.

The variation of F_{NUT} for the non-prismatic member having parabolic haunches and straight haunches is presented in Fig. 10(a) and Fig. 10(b), respectively. From the finite element modeling, it is seen that the fixed-end forces due to linear temperature gradient occur at the ends of the non-prismatic beams. Because of the arching action, a significant amount of fixed-end forces came into existence because of the linear temperature gradient. However, it should be pointed out that the fixed-end forces (F_{NUT}) due to linear temperature gradient were obtained as zero using the available non-prismatic member formulations or available commercial structural analysis programs. The parametric study showed that for a given specific haunch length ratio, the F_{NUT} values increase almost linearly with the increasing haunch depth ratio. However, as the haunch length ratios increase, the increase in the F_{NUT} values decreases with an increasing rate for a given specific haunch depth ratio.

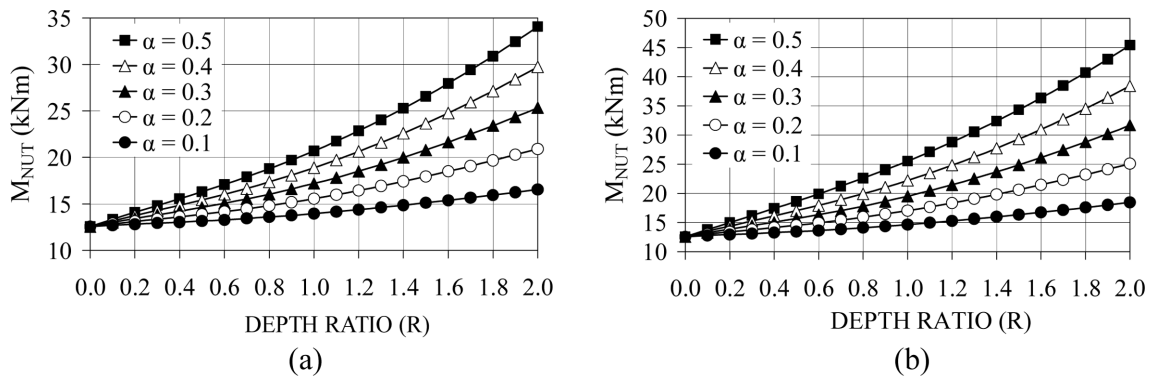


Fig. 11 Variation of the fixed-end moments (M_{NUT}) of the non-prismatic members having (a) parabolic haunches, (b) straight haunches; under the action of linear temperature gradient of ($\Delta T_1 - \Delta T_2 = 1C^\circ$)

Likewise, Fig. 11(a) and Fig. 11(b) illustrate the typical variation of the M_{NUT} of the non-prismatic member having parabolic haunches and straight haunches, respectively. In both cases, the greater the haunch depth ratio the larger the increase in the fixed-end moments due to linear temperature gradient occurred. The relationships between the M_{NUT} values and the haunch depth ratios are non-linear. M_{NUT} values increase as the haunch depth ratios (R) and haunch length ratios (α) are increased. The linear temperature gradient influences the values of F_{NUT} and M_{NUT} for the non-prismatic members with straight haunches more than the values of those for the non-prismatic members with parabolic haunches.

8. Comparison of the finite element analyses' results with the frame element analyses' results

The fixed-end actions of the non-prismatic beams under the actions of the temperature changes were also computed from the structural analysis programs of SAP2000 (CSI 2007a) and ETABS (CSI 2007b) using the non-prismatic frame element modules. The parametric study was performed on the non-prismatic beams having straight and parabolic haunches for different haunch depth ratios ($R = 0.0, 0.1, 0.2, 0.3, 0.4, 0.5, 0.6, 0.7, 0.8, 0.9, 1.0, 1.1, 1.2, 1.3, 1.4, 1.5, 1.6, 1.7, 1.8, 1.9$ and 2.0) and haunch length ratios ($\alpha = 0.1, 0.2, 0.3, 0.4$ and 0.5). In the frame element models, the uniform and non-uniform temperature changes were applied to each non-prismatic beam having parabolic and straight haunches. The uniform temperature changes were applied as a temperature increase of $\Delta T = 1C^\circ$. Non-uniform temperature changes were applied as a linear temperature gradient of $\Delta T_1 - \Delta T_2 = 1C^\circ$ such that the top of the beam had a temperature change of $\Delta T_2 = -0.5$ while the bottom was having a change of $\Delta T_1 = 0.5$ and the temperature at the centroidal axis remained unchanged. The developed fixed-end moments and the fixed-end horizontal forces due to uniform and non-uniform temperature changes were calculated using the frame element models. A uniform temperature change produced only axial forces in the non-prismatic members during the utilization of the frame element model as in the case of the prismatic members as shown in Fig. 2(a). However, from the finite element models in the non-prismatic members, the development of the bending moments was observed in addition to the axial forces. Furthermore, in the frame element models, if a non-prismatic member was subjected to a linear temperature gradient, only the

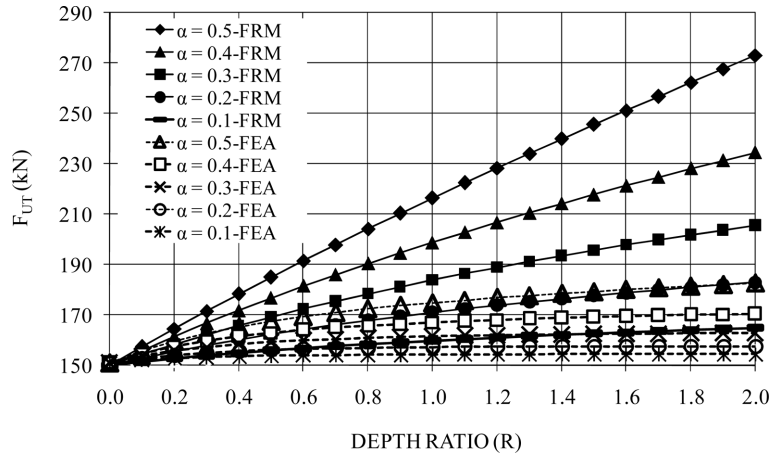


Fig. 12 Comparison of the values of the horizontal reaction forces (F_{UT}) of the non-prismatic members having parabolic haunches which were obtained by the frame element models (FRM) and the finite element analyses (FEA) under the action of uniform temperature increase $\Delta T = 1^\circ\text{C}$

bending moments would be developed similar to the case of the prismatic members as shown in Fig. 2(b). However, the axial force was developed in addition to the bending moments (see Fig. 4(b)) for the same situation of the non-prismatic members in the finite element models.

It should be noted that, the results obtained for the non-prismatic frame elements having parabolic and straight haunches by using SAP2000 (CSI 2007a) and ETABS (CSI 2007b) are the same. Additionally, the fixed-end actions obtained for the non-prismatic members having parabolic haunches and straight haunches by using the frame element models for given haunch depth ratios (R) and haunch length ratios (α) are identical under the conditions of uniform and non-uniform temperature changes. The results of the finite element analyses for non-prismatic members having parabolic haunches are compared with the results of the non-prismatic frame element modulus of SAP2000 (CSI 2007a) in Fig. 12 and Table 1. The results of the finite element analysis and the frame element analysis were denoted as FEA and FRM, respectively. The deviation relative to the finite element analysis results was calculated as in Eq. (3) and the results are presented in Table 1. The F_{UT} and M_{UT} values given in Table 1 for the case of $R = 0.0$ and $\alpha = 0.0$ corresponds to the prismatic members. The results based on the finite element analyses for the F_{UT} and M_{UT} values deviate from those obtained from the theoretical values by a maximum of 0.68% and 0.3%, respectively thereby demonstrating the validity of the results of the finite element analyses.

$$\text{Deviation relative to FEA} = D\% = \left[\frac{\text{FEA} - \text{EFM}}{\text{FEA}} \right] \times 100 \tag{3}$$

From Table 1, it can be seen that there are large discrepancies between the results of the two methods of analyses (FEA and FRM). The deviation in the fixed-end horizontal force values and fixed-end moment values increase as the R and α values increase. As the relative length ratio (α) and the depth ratio (R) increased in both of the frame element modeling and the finite element modeling, the fixed-end horizontal forces increased depending to the uniform temperature increase, thus, in this regard both models became in agreement with each other. However, the fixed-end horizontal forces of the frame element modeling were determined much higher than the fixed-end horizontal forces calculated by the finite element modeling for a given haunch length ratio of α and

Table 1 Deviation relative to FEA = $D\% = [(FEA - EFM) \times FEA] \times 100$ for non-prismatic members having parabolic haunches

| R | F_{UT} | | | | | M_{UT} | | | | |
|-----|----------|--------|--------|--------|--------|----------|-------|-------|-------|--------|
| | α | | | | | α | | | | |
| | 0.1 | 0.2 | 0.3 | 0.4 | 0.5 | 0.1 | 0.2 | 0.3 | 0.4 | 0.5 |
| 0.0 | 0.68 | 0.68 | 0.68 | 0.68 | 0.68 | 0.3 | 0.3 | 0.3 | 0.3 | 0.3 |
| 0.1 | 0.47 | 0.03 | -0.36 | -0.73 | -1.07 | -1.2 | -2.9 | -4.7 | -6.5 | -8.4 |
| 0.2 | 0.09 | -0.83 | -1.67 | -2.43 | -3.15 | -2.7 | -5.9 | -9.5 | -13.5 | -18.1 |
| 0.3 | -0.37 | -1.80 | -3.13 | -4.35 | -5.45 | -3.9 | -8.5 | -13.9 | -20.4 | -28.3 |
| 0.4 | -0.85 | -2.82 | -4.67 | -6.38 | -7.91 | -4.8 | -10.5 | -17.8 | -27.0 | -38.9 |
| 0.5 | -1.34 | -3.84 | -6.24 | -8.48 | -10.46 | -5.4 | -12.0 | -20.9 | -33.0 | -49.8 |
| 0.6 | -1.81 | -4.85 | -7.81 | -10.60 | -13.08 | -5.7 | -12.9 | -23.3 | -38.3 | -60.7 |
| 0.7 | -2.28 | -5.85 | -9.36 | -12.73 | -15.74 | -5.7 | -13.3 | -25.0 | -42.8 | -71.7 |
| 0.8 | -2.72 | -6.82 | -10.89 | -14.85 | -18.42 | -5.4 | -13.2 | -25.9 | -46.5 | -82.4 |
| 0.9 | -3.15 | -7.75 | -12.38 | -16.94 | -21.10 | -4.9 | -12.6 | -26.1 | -49.3 | -93.0 |
| 1.0 | -3.55 | -8.65 | -13.83 | -19.00 | -23.78 | -4.3 | -11.8 | -25.8 | -51.3 | -103.3 |
| 1.1 | -3.94 | -9.51 | -15.24 | -21.02 | -26.45 | -3.4 | -10.5 | -24.8 | -52.5 | -113.4 |
| 1.2 | -4.30 | -10.34 | -16.61 | -23.02 | -29.10 | -2.4 | -9.0 | -23.5 | -53.0 | -123.0 |
| 1.3 | -4.65 | -11.14 | -17.94 | -24.97 | -31.74 | -1.3 | -7.2 | -21.7 | -52.8 | -132.4 |
| 1.4 | -4.98 | -11.91 | -19.23 | -26.88 | -34.35 | -0.1 | -5.3 | -19.6 | -52.1 | -141.4 |
| 1.5 | -5.30 | -12.65 | -20.48 | -28.76 | -36.95 | 1.2 | -3.2 | -17.3 | -50.8 | -150.1 |
| 1.6 | -5.60 | -13.37 | -21.70 | -30.60 | -39.52 | 2.6 | -1.0 | -14.7 | -49.2 | -158.5 |
| 1.7 | -5.90 | -14.06 | -22.87 | -32.40 | -42.07 | 4.0 | 1.2 | -12.1 | -47.1 | -166.6 |
| 1.8 | -6.17 | -14.72 | -24.02 | -34.16 | -44.59 | 5.4 | 3.5 | -9.3 | -44.8 | -174.4 |
| 1.9 | -6.44 | -15.37 | -25.13 | -35.89 | -47.10 | 6.9 | 5.8 | -6.5 | -42.3 | -182.0 |
| 2.0 | -6.70 | -15.98 | -26.22 | -37.59 | -49.58 | 8.4 | 8.1 | -3.6 | -39.5 | -189.4 |

a haunch depth ratio of R . In the frame element modeling, the fixed-end horizontal forces linearly increased with the increasing haunch depth ratios; however, the fixed-end horizontal forces increased non-linearly in the finite element modeling. Deviations for the F_{UT} and M_{UT} values reached to unacceptable levels for the non-prismatic beams with long and deep haunches. The arching action become more important as the haunch length and haunch depth is increased.

9. Design formulas and the empirical design coefficients

Design equations and the design coefficients were developed based on the results of the extensive parametric study with respect to the geometry of the non-prismatic members using two-dimensional plane stress finite element models, which were presented in Section 7. The dimensionless fixed-end action coefficients of $C_{(FUT)}$, $C_{(FNUT)}$, $C_{(MUT)}$ and $C_{(MNUT)}$ were derived by using the values of F_{UT} , F_{NUT} , M_{UT} and M_{NUT} , respectively. The separate design equations were proposed to be able to calculate the horizontal axial forces (Eq. (4)) and the bending moments (Eq. (5)) at the ends of the non-prismatic beams having parabolic and straight haunches subjected to uniform temperature changes. In addition, Eq. (6) and Eq. (7) were also proposed to calculate the horizontal axial forces and the bending moments at the ends of the non-prismatic beams having parabolic and straight

haunches subjected to linear temperature gradients. The proposed method directly gives the design values without performing any additional calculation.

The fixed-end actions at the ends of the non-prismatic beams subjected to uniform temperature changes

$$F_{UT} = C_{FUT} \times E \times A \times \alpha T \times \Delta T \tag{4}$$

$$M_{UT} = (C_{MUT} \times h) \times E \times A \times \alpha T \times \Delta T \tag{5}$$

where,

- F_{UT} : the fixed-end horizontal forces at the ends of the non-prismatic members under uniform temperature changes (ΔT),
- M_{UT} : the fixed-end moments at the ends of the non-prismatic members under uniform temperature changes (ΔT),
- C_{FUT} : the dimensionless coefficient for calculating the fixed-end forces of the non-prismatic members under uniform temperature changes. The C_{FUT} values are given in Table 2 for the non-prismatic members having parabolic and straight haunches.
- C_{MUT} : the dimensionless coefficient for calculating the fixed-end moments of the non-prismatic members under uniform temperature changes. The value of C_{MUT} is determined as

Table 2 Dimensionless coefficients (C_{FUT}) necessary for calculating the fixed-end forces of the non-prismatic members having parabolic and straight haunches due to uniform temperature changes

| R | Parabolic haunch | | | | | Straight haunch | | | | |
|-----|------------------|-------|-------|-------|-------|-----------------|-------|-------|-------|-------|
| | α | | | | | α | | | | |
| | 0.1 | 0.2 | 0.3 | 0.4 | 0.5 | 0.1 | 0.2 | 0.3 | 0.4 | 0.5 |
| 0.0 | 1.007 | 1.007 | 1.007 | 1.007 | 1.007 | 1.007 | 1.007 | 1.007 | 1.007 | 1.007 |
| 0.1 | 1.014 | 1.019 | 1.025 | 1.031 | 1.038 | 1.016 | 1.025 | 1.034 | 1.044 | 1.055 |
| 0.2 | 1.019 | 1.028 | 1.039 | 1.050 | 1.063 | 1.022 | 1.037 | 1.054 | 1.074 | 1.097 |
| 0.3 | 1.022 | 1.034 | 1.049 | 1.065 | 1.084 | 1.026 | 1.045 | 1.068 | 1.097 | 1.134 |
| 0.4 | 1.024 | 1.039 | 1.056 | 1.077 | 1.102 | 1.028 | 1.05 | 1.079 | 1.116 | 1.166 |
| 0.5 | 1.026 | 1.042 | 1.062 | 1.086 | 1.116 | 1.03 | 1.054 | 1.087 | 1.131 | 1.195 |
| 0.6 | 1.027 | 1.044 | 1.066 | 1.094 | 1.129 | 1.031 | 1.056 | 1.092 | 1.143 | 1.221 |
| 0.7 | 1.027 | 1.046 | 1.070 | 1.100 | 1.140 | 1.031 | 1.058 | 1.097 | 1.153 | 1.243 |
| 0.8 | 1.028 | 1.047 | 1.073 | 1.105 | 1.149 | 1.032 | 1.059 | 1.1 | 1.161 | 1.264 |
| 0.9 | 1.029 | 1.048 | 1.075 | 1.110 | 1.158 | 1.032 | 1.06 | 1.102 | 1.167 | 1.282 |
| 1.0 | 1.029 | 1.049 | 1.077 | 1.114 | 1.166 | 1.032 | 1.061 | 1.104 | 1.173 | 1.299 |
| 1.1 | 1.029 | 1.050 | 1.078 | 1.117 | 1.172 | 1.032 | 1.061 | 1.106 | 1.177 | 1.314 |
| 1.2 | 1.029 | 1.050 | 1.080 | 1.120 | 1.179 | 1.032 | 1.061 | 1.107 | 1.181 | 1.328 |
| 1.3 | 1.030 | 1.051 | 1.081 | 1.123 | 1.185 | 1.032 | 1.061 | 1.108 | 1.184 | 1.34 |
| 1.4 | 1.030 | 1.051 | 1.082 | 1.125 | 1.190 | 1.031 | 1.061 | 1.109 | 1.187 | 1.352 |
| 1.5 | 1.030 | 1.051 | 1.083 | 1.128 | 1.195 | 1.031 | 1.061 | 1.11 | 1.19 | 1.363 |
| 1.6 | 1.030 | 1.051 | 1.084 | 1.130 | 1.200 | 1.031 | 1.061 | 1.111 | 1.192 | 1.373 |
| 1.7 | 1.030 | 1.052 | 1.084 | 1.132 | 1.205 | 1.031 | 1.061 | 1.111 | 1.194 | 1.382 |
| 1.8 | 1.030 | 1.052 | 1.085 | 1.133 | 1.209 | 1.031 | 1.061 | 1.112 | 1.196 | 1.39 |
| 1.9 | 1.030 | 1.052 | 1.085 | 1.135 | 1.213 | 1.031 | 1.061 | 1.112 | 1.198 | 1.398 |
| 2.0 | 1.030 | 1.052 | 1.086 | 1.137 | 1.217 | 1.031 | 1.06 | 1.113 | 1.2 | 1.405 |

$(0.534 \times R)$ for non-prismatic beams having parabolic and straight haunches.

- E : the modulus of elasticity;
- A : the cross-sectional area at the mid-span of the non-prismatic members;
- h : the mid-span or minimum depth of the non-prismatic members, h is 1.0 m for this parametric study;
- αT : the coefficient of thermal expansion;
- ΔT : uniform temperature change;

The fixed-end actions at the ends of the non-prismatic members subjected to linear temperature gradient $(\Delta T_1 - \Delta T_2)$

$$F_{NUT} = \left[\frac{C_{FNUT}}{h} \right] \times \frac{\alpha T \times E \times I \times (\Delta T_1 - \Delta T_2)}{h} \tag{6}$$

$$M_{NUT} = C_{MNUT} \times \frac{\alpha T \times E \times I \times (\Delta T_1 - \Delta T_2)}{h} \tag{7}$$

where,

- F_{NUT} : the fixed-end horizontal forces at the ends of the non-prismatic members under linear temperature gradient $(\Delta T_1 - \Delta T_2)$,

Table 3 Dimensionless coefficients (C_{FNUT}) necessary for calculating the fixed-end forces of the non-prismatic members having parabolic and straight haunches due to linear temperature gradient $(\Delta T_1 - \Delta T_2 = 1C^\circ)$

| R | Parabolic haunch | | | | | Straight haunch | | | | |
|-----|------------------|-------|-------|-------|-------|-----------------|-------|-------|-------|-------|
| | α | | | | | α | | | | |
| | 0.1 | 0.2 | 0.3 | 0.4 | 0.5 | 0.1 | 0.2 | 0.3 | 0.4 | 0.5 |
| 0.0 | 0.000 | 0.000 | 0.000 | 0.000 | 0.000 | 0.000 | 0.000 | 0.000 | 0.000 | 0.000 |
| 0.1 | 0.003 | 0.007 | 0.009 | 0.010 | 0.011 | 0.006 | 0.011 | 0.013 | 0.013 | 0.010 |
| 0.2 | 0.014 | 0.025 | 0.033 | 0.038 | 0.039 | 0.024 | 0.039 | 0.048 | 0.048 | 0.039 |
| 0.3 | 0.029 | 0.051 | 0.067 | 0.077 | 0.080 | 0.048 | 0.079 | 0.098 | 0.101 | 0.083 |
| 0.4 | 0.047 | 0.081 | 0.107 | 0.125 | 0.131 | 0.075 | 0.125 | 0.158 | 0.168 | 0.139 |
| 0.5 | 0.065 | 0.113 | 0.152 | 0.179 | 0.189 | 0.104 | 0.175 | 0.226 | 0.244 | 0.206 |
| 0.6 | 0.084 | 0.147 | 0.199 | 0.237 | 0.253 | 0.133 | 0.228 | 0.299 | 0.328 | 0.282 |
| 0.7 | 0.102 | 0.181 | 0.247 | 0.297 | 0.319 | 0.162 | 0.281 | 0.374 | 0.418 | 0.365 |
| 0.8 | 0.120 | 0.214 | 0.296 | 0.358 | 0.389 | 0.190 | 0.334 | 0.450 | 0.510 | 0.454 |
| 0.9 | 0.138 | 0.248 | 0.345 | 0.420 | 0.460 | 0.218 | 0.387 | 0.526 | 0.605 | 0.547 |
| 1.0 | 0.155 | 0.281 | 0.393 | 0.482 | 0.531 | 0.244 | 0.438 | 0.601 | 0.701 | 0.644 |
| 1.1 | 0.171 | 0.313 | 0.441 | 0.544 | 0.603 | 0.269 | 0.488 | 0.676 | 0.797 | 0.744 |
| 1.2 | 0.187 | 0.344 | 0.488 | 0.605 | 0.675 | 0.293 | 0.537 | 0.749 | 0.892 | 0.846 |
| 1.3 | 0.202 | 0.374 | 0.533 | 0.665 | 0.747 | 0.315 | 0.584 | 0.820 | 0.987 | 0.950 |
| 1.4 | 0.216 | 0.404 | 0.578 | 0.724 | 0.818 | 0.337 | 0.630 | 0.890 | 1.080 | 1.055 |
| 1.5 | 0.230 | 0.432 | 0.622 | 0.783 | 0.889 | 0.358 | 0.673 | 0.958 | 1.172 | 1.161 |
| 1.6 | 0.243 | 0.460 | 0.665 | 0.840 | 0.959 | 0.377 | 0.716 | 1.024 | 1.263 | 1.267 |
| 1.7 | 0.256 | 0.487 | 0.706 | 0.896 | 1.028 | 0.396 | 0.757 | 1.089 | 1.352 | 1.373 |
| 1.8 | 0.268 | 0.513 | 0.747 | 0.951 | 1.096 | 0.414 | 0.796 | 1.151 | 1.439 | 1.480 |
| 1.9 | 0.280 | 0.538 | 0.786 | 1.005 | 1.163 | 0.430 | 0.834 | 1.212 | 1.525 | 1.586 |
| 2.0 | 0.291 | 0.562 | 0.824 | 1.058 | 1.229 | 0.447 | 0.871 | 1.272 | 1.608 | 1.692 |

- M_{NUT} : the fixed-end moments at the ends of the non-prismatic members subjected to linear temperature gradient ($\Delta T_1 - \Delta T_2$),
- C_{FNUT} : the dimensionless coefficient for calculating the fixed-end forces of the non-prismatic members subjected to linear temperature gradient. The values of C_{FNUT} are given in Table 3 for the non-prismatic members having parabolic and straight haunches.
- C_{MNUT} : the dimensionless coefficient for calculating the fixed-end moments of the non-prismatic members subjected to linear temperature gradient. The values of C_{MNUT} are given in Table 4 for the non-prismatic members having parabolic and straight haunches.
- ΔT_1 : the temperature change at the bottom of the beam,
- ΔT_2 : the temperature change at the top of the beam,
- $(\Delta T_1 - \Delta T_2)$: the linear temperature gradient such that the top of the beam has a temperature change of ΔT_2 while the bottom has a change of ΔT_1 and the temperature at the centroidal axis remains unchanged.
- I : the moment of inertia at the mid-span of the non-prismatic members;

Table 4 Dimensionless coefficients (C_{MNUT}) necessary for calculating the fixed-end forces of the non-prismatic members having parabolic and straight haunches due to linear temperature gradient ($\Delta T_1 - \Delta T_2 = 1\text{C}^\circ$)

| R | Parabolic haunch | | | | | Straight haunch | | | | |
|-----|------------------|-------|-------|-------|-------|-----------------|-------|-------|-------|-------|
| | α | | | | | α | | | | |
| | 0.1 | 0.2 | 0.3 | 0.4 | 0.5 | 0.1 | 0.2 | 0.3 | 0.4 | 0.5 |
| 0.0 | 1.003 | 1.003 | 1.003 | 1.003 | 1.003 | 1.003 | 1.003 | 1.003 | 1.003 | 1.003 |
| 0.1 | 1.016 | 1.028 | 1.041 | 1.054 | 1.067 | 1.021 | 1.040 | 1.060 | 1.080 | 1.102 |
| 0.2 | 1.025 | 1.049 | 1.073 | 1.100 | 1.127 | 1.035 | 1.071 | 1.110 | 1.152 | 1.199 |
| 0.3 | 1.034 | 1.068 | 1.105 | 1.144 | 1.186 | 1.048 | 1.101 | 1.158 | 1.221 | 1.295 |
| 0.4 | 1.042 | 1.088 | 1.136 | 1.188 | 1.244 | 1.061 | 1.130 | 1.205 | 1.290 | 1.392 |
| 0.5 | 1.052 | 1.109 | 1.169 | 1.233 | 1.304 | 1.075 | 1.161 | 1.254 | 1.361 | 1.490 |
| 0.6 | 1.062 | 1.132 | 1.204 | 1.281 | 1.366 | 1.091 | 1.195 | 1.307 | 1.434 | 1.592 |
| 0.7 | 1.074 | 1.157 | 1.242 | 1.333 | 1.432 | 1.108 | 1.232 | 1.363 | 1.512 | 1.697 |
| 0.8 | 1.087 | 1.184 | 1.283 | 1.388 | 1.502 | 1.128 | 1.272 | 1.424 | 1.595 | 1.807 |
| 0.9 | 1.101 | 1.213 | 1.327 | 1.447 | 1.576 | 1.149 | 1.316 | 1.489 | 1.683 | 1.922 |
| 1.0 | 1.116 | 1.245 | 1.375 | 1.510 | 1.655 | 1.172 | 1.363 | 1.560 | 1.777 | 2.042 |
| 1.1 | 1.132 | 1.279 | 1.426 | 1.578 | 1.740 | 1.196 | 1.414 | 1.636 | 1.877 | 2.169 |
| 1.2 | 1.150 | 1.315 | 1.481 | 1.650 | 1.829 | 1.222 | 1.468 | 1.716 | 1.984 | 2.303 |
| 1.3 | 1.168 | 1.353 | 1.538 | 1.727 | 1.923 | 1.250 | 1.525 | 1.802 | 2.098 | 2.443 |
| 1.4 | 1.188 | 1.393 | 1.599 | 1.807 | 2.022 | 1.279 | 1.585 | 1.893 | 2.218 | 2.590 |
| 1.5 | 1.208 | 1.435 | 1.663 | 1.892 | 2.127 | 1.309 | 1.649 | 1.989 | 2.344 | 2.745 |
| 1.6 | 1.230 | 1.479 | 1.730 | 1.982 | 2.237 | 1.340 | 1.715 | 2.089 | 2.477 | 2.907 |
| 1.7 | 1.252 | 1.525 | 1.800 | 2.075 | 2.352 | 1.373 | 1.784 | 2.194 | 2.616 | 3.077 |
| 1.8 | 1.275 | 1.573 | 1.873 | 2.172 | 2.472 | 1.407 | 1.856 | 2.303 | 2.762 | 3.254 |
| 1.9 | 1.299 | 1.622 | 1.948 | 2.273 | 2.596 | 1.441 | 1.930 | 2.416 | 2.914 | 3.439 |
| 2.0 | 1.323 | 1.673 | 2.027 | 2.378 | 2.726 | 1.477 | 2.006 | 2.534 | 3.072 | 3.632 |

The C_{FUT} , C_{FNUT} and C_{MNUT} coefficients are the functions of the haunch depth ratios (R) and the haunch length ratios (α). The design coefficients of C_{FUT} , C_{FNUT} and C_{MNUT} were proposed for different haunch depth ratios ($R = 0.0, 0.1, 0.2, 0.3, 0.4, 0.5, 0.6, 0.7, 0.8, 0.9, 1.0, 1.1, 1.2, 1.3, 1.4, 1.5, 1.6, 1.7, 1.8, 1.9$ and 2.0) and haunch length ratios ($\alpha = 0.1, 0.2, 0.3, 0.4$ and 0.5). However, it should be pointed out that the most important factor in determining the C_{MUT} coefficient is the haunch depth ratio (R). In this paper, all the design coefficients were obtained from the finite element models and the linear interpolation can be done between the C_{FUT} , C_{FNUT} , C_{MNUT} values. The proposed Eqs. (4), (5), (6) and (7) can be used to obtain more rigorous estimates of the fixed-end forces and the fixed-end moments at the ends of the non-prismatic members under temperature changes without necessitating any finite element analysis. It is also worth mentioning that the empirical coefficients are dimensionless, and the consistent units given in this paper should be used for their applications.

10. Conclusions

In this paper, the linear elastic behavior of the non-prismatic members subjected to uniform and non-uniform temperature changes was studied by using the plane stress finite elements. Since concrete's modulus of elasticity and poisson ratio are considered in the analyses, all of the results obtained in this study are valid for the structures made of concrete. An extensive parametric study was conducted and the fixed-end actions acting at the ends of the restrained non-prismatic members having parabolic and linear height variations under temperature changes were computed employing the finite element method. The uniform temperature changes were applied along the beam length. The non-uniform temperature changes were applied as a linear temperature gradient such that the top surface of the beam would have a temperature change of ΔT_2 , while the bottom surface would have a change of ΔT_1 and the temperature at the centroidal axis remains unchanged. The parametric studies were performed for the non-prismatic members ($b = 0.5$ m, $h = 1$ m, $L = 10$ m) having haunch depth ratios (R) varying in the range of 0.0 to 2.0 with an interval of 0.1 and for the haunch length ratios of $\alpha = 0.1, 0.2, 0.3, 0.4$ and 0.5 by using the realistic theoretical models. F_{UT} , F_{NUT} , M_{UT} and M_{NUT} values were calculated for the non-prismatic members having various haunch depth ratios (R) and haunch length ratios (α).

Based on the present finite element analyses' results, the design formulas (Eqs. (4), (5), (6) and (7)) and the design coefficients (Tables 2, 3 and 4) were proposed to be able to compute the design forces at the ends of the non-prismatic members subjected to temperature changes without necessitating any finite element analyses. The design coefficients were separately proposed as the functions of the haunch depth ratios (R) and the haunch length ratios (α) for the uniform and the non-uniform temperature changes. The formulation includes the shape of the cross-section of the non-prismatic members, the discontinuity of the centroidal axis, the local stress concentrations, the nonlinear stress distributions and the existence of the null areas that reduces the member stiffness. The presented results are valid only for the non-prismatic members having symmetrical parabolic and straight haunches ($b = 0.5$ m, $h = 1$ m, $L = 10$ m); however, the approach can be easily expanded to cover the non-prismatic members having non-symmetrical haunches.

It is demonstrated that the fixed-end actions for the non-prismatic members under uniform and non-uniform temperature changes are greatly influenced by the geometric parameters of the R and α . Thus, they are important in the arch formation and affect in turn the location of the arch height,

the axial thrust values and the bending moments. Under uniform temperature changes, considerable amount of bending moments occurred in addition to the horizontal forces. The analytical approaches and the traditional beam theories often need to introduce assumptions to simplify the problem and yield an erroneous solution. Unless the detailed finite element modeling is utilized, the current conventional methods using frame elements will become deficient to compute these forces due to the progressive change of the centroidal axis associated with the non-prismatic sections. The writer recommends using the finite element analysis results by considering the coupling effect completely as well as the stress distributions rather than using the conventional method of analysis with large deviations, as shown in this study.

References

- Al-Gahtani, H.J. (1996), "Exact stiffnesses for tapered members", *J. Struct. Eng.*, ASCE, **122**(10), 1234-1239.
- Balkaya, C. (2001), "Behavior and modeling of nonprismatic members having T-sections", *J. Struct. Eng.*, ASCE., **127**(8), 940-946.
- Balkaya, C., Kalkan, E. and Yuksel, S.B. (2006), "FE analysis and practical modeling of RC multi-bin circular silos", *ACI Struct. J.*, **103**(3), 365-371.
- Bathe, K.J. (1996), *Finite Element Procedures*. Prentice Hall Publisher, NJ, USA.
- Brown, C.J. (1984), "Approximate stiffness matrix for tapered beams", *J. Struct. Eng.*, ASCE, **110**(12), 3050-3055.
- CSI (2007a), Computer and Structures Inc. SAP2000 User's Manual. Berkeley, CA.
- CSI (2007b), Computer and Structures Inc. ETABS User's Manual. Berkeley, CA.
- Eisenberger, M. (1985), "Explicit Stiffness matrices for non-prismatic members", *Comput. Struct.*, **20**(4), 715-720.
- Eisenberger, M. (1991), "Stiffness matrices for non-prismatic members including transverse shear", *Comput. Struct.*, **40**(4), 831-835.
- El-Mezaini, N., Balkaya, C. and Citipitioglu, E. (1991), "Analysis of frames with nonprismatic members", *J. Struct. Eng.*, ASCE., **117**(6), 1573-1592.
- Friedman, Z. and Kosmatka, J.B. (1992a), "Exact stiffness matrix of a non-uniform beam-I. Extension, torsion, and bending of a Bernoulli-Euler beam", *Comput. Struct.*, **42**(5), 671-682.
- Friedman, Z. and Kosmatka, J.B. (1992b), "Exact stiffness matrix of a non-uniform beam-II. Bending of a Timoshenko beam", *Comput. Struct.*, **49**(3), 545-555.
- Funk, R.R. and Wang, K.T. (1988), "Stiffness of non-prismatic members", *J. Struct. Eng.*, ASCE, **114**(2), 489-494.
- Hibbeler, R. (2002), *Structural analysis*, Prentice-Hall, Inc., Fifth Edition, Upper Saddle River, New Jersey 07548.
- Horowitz, B. (1997), "Singularities in elastic finite element analysis", *Concrete Int.*, December, 33-36.
- Hu, X.M., Zheng, D.S. and Yang, L. (2006), "Experimental behaviour of extended end-plate composite beam-to-column joints subjected to reversal of loading", *Struct. Eng. Mech.* **24**(3), 307-321.
- Lee, C.H., Jung, J.H., Oh, M.H. and Koo, E. (2003), "Cyclic seismic testing of steel moment connections reinforced with welded straight haunch", *Eng. Struct.*, **25**(14), 1743-1753.
- Maugh, L.C. (1964), *Statically Indeterminate Structures: Continuous Girders and Frames with Variable Moment of Inertia*, John&Wiley, New York, 202-243.
- Medwadowski, S.J. (1984), "Nonprismatic shear beams", *J. Struct. Eng.*, ASCE, **110**(5), 1067-1082.
- Oh, S.H., Kim, Y.J. and Moon, T.S. (2007), "Cyclic performance of existing moment connections in steel retrofitted with a reduced beam section and bottom flange reinforcements", *Can. J. Civ. Eng.*, **34**(2), 199-209.
- Ozay, G. and Topcu, A. (2000), "Analysis of frames with non-prismatic members", *Can. J. Civ. Eng.*, **27**, 17-25.
- Pampanin, S., Christopoulos, C. and Chen, T.H. (2006), "Development and validation of a metallic haunch seismic retrofit solution for existing under-designed RC frame buildings", *Earthq. Eng. Struct. D.*, **35**(14),

- 1739-1766.
- Portland Cement Association (PCA) (1958), "Beam factors and moment coefficients for members of variable cross-section", Handbook of frame constants, Chicago.
- Shanmugam, N.E., Ng, Y.H. and Liew, J.Y.R. (2002), "Behaviour of composite haunched beam connection", *Eng. Struct.*, **24**(11), 1451-1463.
- Tanaka, N. (2003), "Evaluation of maximum strength and optimum haunch length of steel beam-end with horizontal haunch", *Eng. Struct.*, **25** (2), 229-239.
- Tartaglione, L.C. (1991), *Structural Analysis*, McGraw-Hill, Ins., United States of America.
- Tena-Colunga, A. (1996), "Stiffness formulation for nonprismatic beam elements", *J. Struct. Eng.*, ASCE, **122**(12), 1484-1489.
- Timoshenko, S.P. and Young, D.H. (1965), *Theory of Structures*, McGraw-Hill Book Co., Inc., New York, USA.
- Valderbilt, M.D. (1978), "Fixed-end action and stiffness matrices for non-prismatic beams", *J. Am. Concr. Inst.*, **75**(1), 290-298.
- Weaver, W. and Gere, J.M. (1990), *Matrix Analysis of Framed Structures*, Van Nostrand Reinhold, New York.
- Yuksel, S.B. (2008) "Slit connected coupling beams for tunnel form building structures", *J. Struct. Des. Tall Spec.*, **17**(3), 579-600. DOI: 10.1002/tal.367.
- Yuksel S.B. and Arikan S. (2009), "A new set of design aids for the groups of four cylindrical silos due to interstorey and internal loadings", *J. Struct. Des. Tall Spec.*, DOI: 10.1002/tal.399.